

Hemagglutination Mediated by SARS-CoV-2 Spike Protein

Subjects: [Biochemistry & Molecular Biology](#)

Contributor: david schein

Although COVID-19 typically gains infectious penetration in the respiratory epithelium, vascular damage is frequently observed in lungs and other organ systems of COVID-19 patients, with morbidities such as intravascular clotting, microvascular occlusion and peripheral ischemia. The arrangement and chemical composition of the glycans at the 22 N-glycosylation sites of SARS-CoV-2 spike protein and those at the sialoglycoprotein coating of RBCs allow exploration of specifics as to how virally induced RBC clumping may form. The in vitro and clinical testing of these possibilities can be sharpened by the incorporation of an existing anti-COVID-19 therapeutic that has been found in silico to competitively bind to multiple glycans on SARS-CoV-2 spike protein.

SARS-CoV-2

spike protein

COVID-19

betacoronavirus

sialic acid

glycophorin A

CD147

hemagglutination

hemagglutinin esterase

α 5-N-acetylneuraminic acid (Neu5Ac)

1. Introduction

Although COVID-19 typically gains infectious penetration in the respiratory epithelium ^{[1][2][3]}, vascular damage is frequently observed in lungs and other organ systems of COVID-19 patients, with morbidities such as intravascular clotting, microvascular occlusion and peripheral ischemia ^{[4][5][6][7][8][9][10][11][12][13][14][15][16][17]}. Histological studies from COVID-19 patients have found extensively damaged endothelium of pulmonary capillaries adjoining relatively intact alveoli ^{[18][19]}, corresponding to hypoxemia with normal breathing mechanics observed in patients with this viral disease ^{[10][16][17][18][20][21]}. One clinical reviewer characterized COVID-19 as “a systemic disease that primarily injures the vascular endothelium” ^[21].

A framework for studying the vascular occlusive morbidities characteristic of COVID-19 is provided by viral properties dating back to classic experiments of the 1940s, as reviewed ^[22]. Viruses fuse and then replicate via host cell receptors specific to the viral strain, which is ACE2 for SARS-CoV-2 ^{[23][24]}. However, many enveloped viral strains, including coronaviruses, initially attach to host cell membranes via glycoconjugate molecules, including those tipped with sialic acid (SA) ^{[25][26][27][28][29][30]}. SA is densely distributed on red blood cells (RBCs) as terminal residues of its surface sialoglycoprotein, glycophorin A (GPA), and of its CD147 transmembrane receptors ^{[31][32][33][34]}. Through viral bindings to SA surface moieties to be considered in detail below, SARS-CoV-2 agglutinates RBCs, as established in vitro ^[35], with such bindings also demonstrated clinically ^[36]. Hemagglutination also occurs for several other viral strains including other coronaviruses ^{[35][37][38][39][40][41][42][43][44][45][46][47][48]}, as demonstrated in the classic viral hemagglutination assay. In that assay, developed in the 1940s ^[38]

[49][50][51] and refined later by Jonas Salk [52][53][54][55][56], virus particles are mixed with RBCs to form a hemagglutinated sheet [40][57][58][59]. However, for viruses that express enzymes that cleave SA, that sheet subsequently collapses as these enzymes disintegrate SA-binding sites on the RBCs [38][58][60][61]. **Figure 1** shows a schematic of virally mediated hemagglutination and of its inhibition through an agent that competitively binds to attachment sites on the virus, in this case an antiviral antibody.

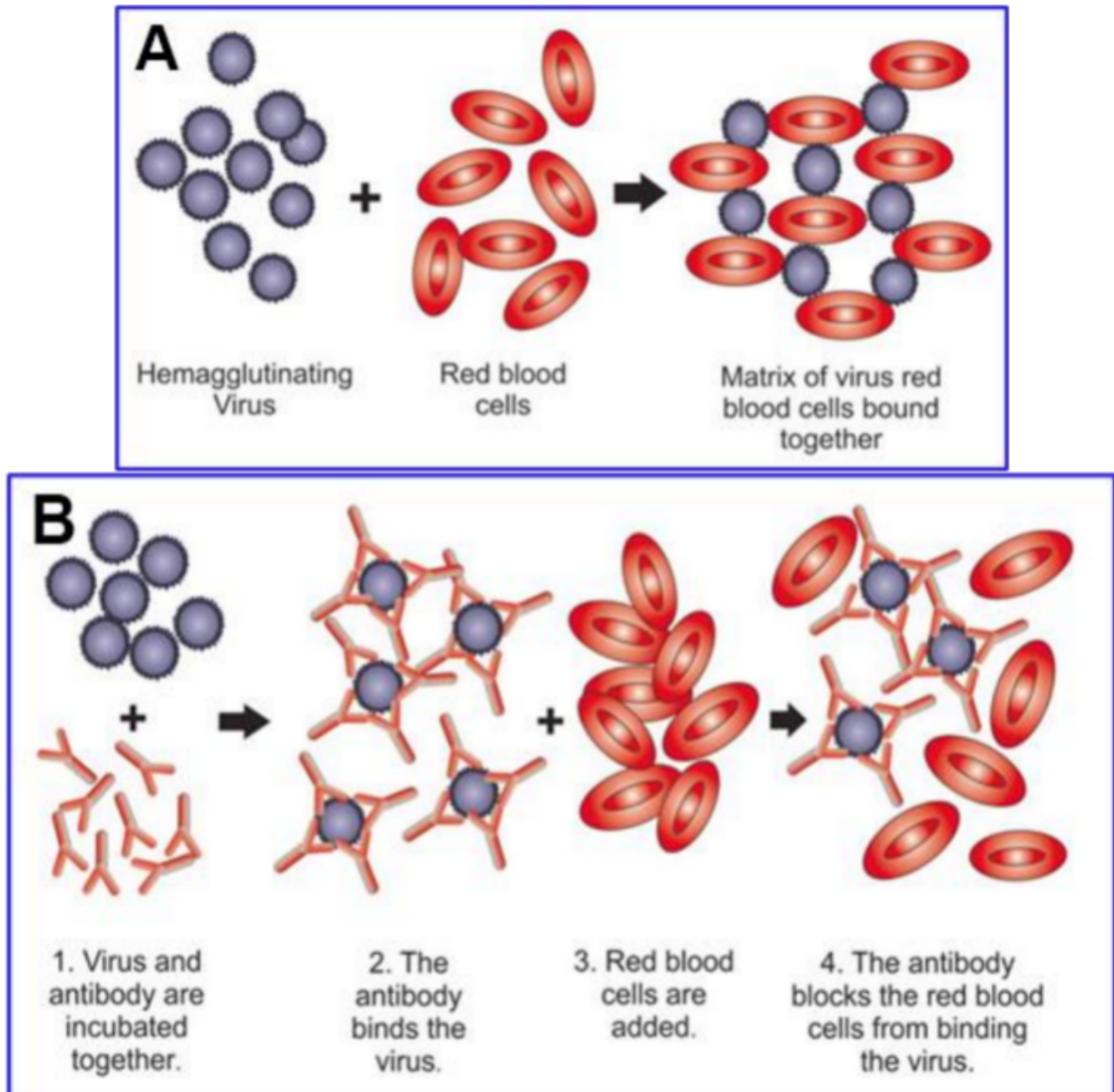


Figure 1. Schematic of hemagglutination (A) and hemagglutination inhibition (B), both of which occur either in vitro in their respective assays or in vivo. Reproduced with permission from Springer Nature ((A) Killian, 2014 [57]; (B) Pedersen, 2014 [60]). (B) depicts blockage of hemagglutination by an antibody to the virus.

1.1. Binding of Viruses to SA and Host Decoy Defense

For viruses that bind to SA, including SARS-CoV-2 as noted above, such glycan bindings play a key role in viral infectivity, as SA typically functions as an initial point of attachment to host cells [25][30][44][48][62][63][64][65][66][67][68][69][70]. The human host, reciprocally, protects against attachment of virions to host cell infectious targets by presenting SA on a set of decoys, including RBCs as well as platelets and leukocytes [22][31][71][72][73]. In particular, SA moieties are densely distributed on the RBC surface (35 million per cell [33]), mainly as terminal residues of both the CD147 receptor [22] and GPA [31][74], with GPA serving no known physiological role other than as a decoy for pathogens [31][72][73][75]. RBCs perform an active pathogen clearance role, attaching to microorganisms and then delivering them to leukocytes or conveying them to macrophages in the liver or spleen for phagocytosis [31][71][73][76]. With bacteria, this clearance by RBCs requires both antibody and complement [77][78]. Viruses, however, are snagged directly by RBCs, and viral–RBC binding is inhibited by antiviral antibodies [22]. RBCs are well suited for this immune defense role, having no nucleus or other infrastructure to perform viral replication and being expendable, numbering 20–30 trillion per human host [72].

1.2. Cleavage of Viral–SA Binding via Hemagglutinin Esterase (HE), an Enzyme Expressed by the Common Cold Betacoronavirus Strains but Not by SARS-CoV, SARS-CoV-2 and MERS

Hemagglutinin esterase (HE) is an SA-cleaving enzyme deployed by certain viral strains, including some betacoronaviruses. HE increases the infectivity of these viral strains by expediting the release of replicated virions from sialoside-binding sites on host cells and by restricting viral snagging on such binding sites of non-infectious targets, including mucins, blood cells and plasma proteins [22]. Viral HE can both bond and cleave host cell sialoside-binding sites [79][80]; however, for betacoronaviruses, even for those expressing HE, attachments to host cell sialoside-binding sites are effected mainly through glycans at 22 N-glycosylation sites on viral spike protein S1, in particular, eight of those clustered on the N-terminal domain (NTD) [44][81][82][83][84][85][86][87]. Genomic analysis of the five strains of human betacoronaviruses reveals expression of the HE enzyme in those that cause the common cold, OC43 and HKU1, but not in the three deadly strains, SARS-CoV, SARS-CoV-2 and MERS [88][89][90][91][92].

1.3. Multivalent Binding

To adjust for a missing release capability in the three betacoronavirus strains lacking HE, SA-binding affinity is diminished, while multiplicity of binding provides robust variations in attachment strength [44][48][62][63][93][94]. These viral bonds to SA and other glycans have weak individual affinities but greatly increased collective strength [25][30][44][48][63][66][93][94][95][96]. The dissociation constant K_d for a multivalent attachment of viral spike protein to SA increases exponentially (in absolute value) as a function of the number of bonds [97][98]. For example, the K_d of an individual bond of viral spike protein to a host sialoside-binding site is in the low millimolar range [63][93][99][100], but the K_d value would be in the nanomolar range for a triple bond [97]. A single sialoside bond for a virus particle initially attaching to a cell would provide only a tentative foothold [25][30][44][63][101][102], allowing migration to an ACE2 receptor for fusion and replication.

2. Properties of SARS-CoV-2 Related to Its Array of Spike Glycoprotein Glycans

2.1. SARS-CoV-2 Binds to SA and CD147

Because bindings from viral spike protein to SA are generally weak when univalent, several coronavirus strains require a nanoarray experimental detection methodology to register viral attachment to hosts [22][48][61][62]. Using such a methodology, a nanoparticle array bearing SA derivatives, the binding of both SARS-CoV-2 spike protein and pseudovirus was demonstrated [94]. This entry's detection system is adaptable to mass COVID-19 screening, with a 5 nM concentration threshold for detection of viral spike protein. Another attachment point on host cells for the SARS-CoV-2 virus is the CD147 transmembrane receptor, which contains SA at its terminal domains [34][103]. Binding of SARS-CoV-2 spike protein to CD147 was shown by enzyme-linked immunosorbent assay (ELISA), surface plasmon resonance (SPR) and co-immunoprecipitation (Co-IP) assays, and colocalization of CD147 and viral spike protein was revealed on infected Vero E6 cells [104]. Meplazumab, a humanized anti-CD147 antibody, was found to inhibit viral proliferation in vitro and to provide significant clinical benefits in a small study of its use for COVID-19 treatment [105].

2.2. SARS-CoV-2 Attaches to RBCs, Other Blood Cells and Endothelial Cells

Several of the glycans at the 22 N-glycosylation sites and both O-linked glycans on SARS-CoV-2 spike protein (as depicted in Figure 3) are capped with SA monosaccharides of the same type that are densely distributed on human RBCs at the tips of GPA molecules, as will be considered in some detail below. These matching glycans enable SARS-CoV-2 to hemagglutinate when mixed with human RBCs, as indeed demonstrated using the hemadsorption assay [35] (similar to the hemagglutination assay [106][107]). Hemagglutination occurs more generally in eight families of viruses, including other coronaviruses [35][37][38][39][40][41][42][43][44][45][46][47][48]. Attachment of SARS-CoV-2 spike protein to RBCs was demonstrated directly through immunofluorescence analysis of RBCs from the blood of nine hospitalized COVID-19 patients [36]. The mean percentage of RBCs having SARS-CoV-2 spike protein punctae was 41% at day 0 of hospital admission, with values ranging from 0% for one patient and 18% for two patients to 79% for another patient. This mean percentage increased to 44% at day 7 after hospital admission.

Like RBCs, several other cell types express surface SA glycoconjugates and can thus also attach to SARS-CoV-2 virus particles. SA and SA-tipped CD147 are expressed on endothelial cells of blood vessel linings (luminal surface), platelets, lymphocytes, macrophages, and other types of white blood cells [22]. The potential for pathogen attachments to SA and CD147 that impede vascular blood flow is indicated in another disease, severe malaria, in which the malaria parasite attaches to SA-binding sites on an RBC [73][108][109] and penetrates the RBC through the latter's CD147 receptors [110][111]. Clumps develop between infected and uninfected RBCs, often including platelets, which, along with endothelial cytoadhesion by infected RBCs, cause vascular occlusion, the key morbidity of severe malaria [22].

The interlaced attachments of RBCs with SARS-CoV-2 virions as observed in vitro in the hemadsorption assay [35] may well define the mechanism by which clumps (rouleaux) of RBCs form in the blood of COVID-19 patients [112][113][114], as shown in **Figure 2**. These clumps would present vascular obstructive potential, given that an RBC of average disk diameter 8 μm [115][116] traverses through an alveolar capillary of smaller average cross-sectional diameter [117], achieved only by a distortion of the RBC's shape to press against the capillary wall [116][118]. Such RBC clumps could be a prime cause of the microvascular occlusion which, as noted above, is characteristic of COVID-19. These clumps could contribute as well to microvascular occlusion in larger capillaries, of cross-sectional diameter up to 20 μm [115][119], elsewhere in the body. Vascular occlusion would be promoted even though such stacked RBC clumps (rouleaux) typically dynamically aggregate and disaggregate [120][121][122], as do RBC aggregates that can form in the absence of pathogens, promoted by macromolecules in plasma under conditions of low blood shear rates [123][124]. Formation of RBC rouleaux would increase blood viscosity [121][122], impeding blood flow, especially in the small-diameter pulmonary capillaries, which would cascade as reduction in both flow velocity and associated shear forces would in turn tend to favor aggregation vs. disaggregation and further occlude flow [121].

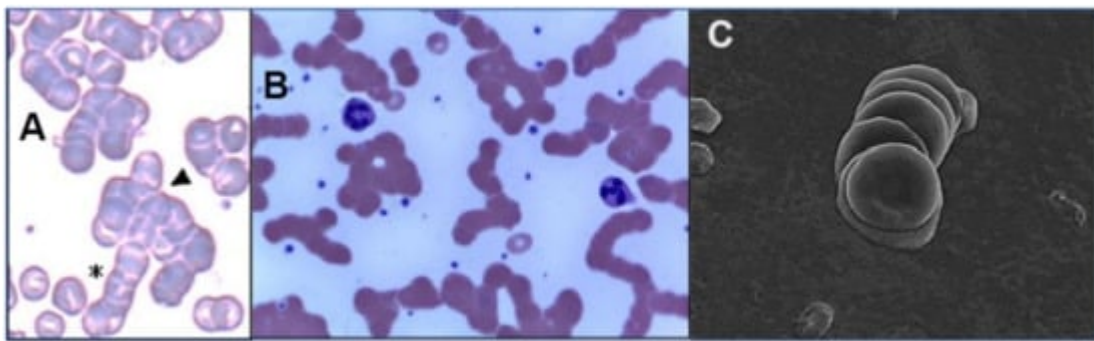


Figure 2. Images of RBC rouleaux (clumps) from the blood of COVID-19 patients, obtained using light ((A) [112], (B) [113]) and electron microscopy ((C) [114]). The first study (A) found huge rouleaux formation by RBCs in 85% of COVID-19 patients studied [112]; the second (B) found these in 33% of patients [113]; and the third (C) found these prevalent in its series of 31 patients, all with mild COVID-19 [114]. Reproduced with permission from (A) SIMTIPRO Srl; (B) CC-BY 4.0; (C) Georg Thieme Verlag KG.

The abundant distribution of SA-tipped CD147 on endothelial cells of blood vessel linings, with 28,000 CD147 receptors (vs. 175 ACE2 receptors) per endothelial cell [125], may be key to the attachments of SARS-CoV-2 to endothelium and the ensuing damage that has been widely observed in COVID-19 patients [15][18][19][126][127][128]. Damage to endothelium caused by SARS-CoV-2 spike protein in the absence of whole virus was demonstrated both in vitro and in vivo in three studies [129][130][131], and presence of isolated SARS-CoV-2 spike protein on endothelial cells was also observed clinically [130][132][133][134][135]. Additionally, one study of 31 hospitalized patients with mild to moderate COVID-19 found that serum levels of circulating endothelial cells (CECs), as determined by different measures, were up to 100-fold the levels for matched controls, and that these CECs from the COVID-19 patients typically each had several holes in their membranes approximately the size of SARS-CoV-2 viral capsid (the viral envelope) [114].

2.3. The Glycan Distribution and Composition at the 22 N-Glycosylation Sites of SARS-CoV-2 Spike Protein

To explore key characteristics of glycan-mediated SARS-CoV-2 spike protein binding to host cells, it is helpful to consider the specific distribution and composition of the glycans at its glycosylation sites. SARS-CoV-2 spike glycoprotein is a trimer with a central helical stalk embedded in the viral envelope at its C-terminal end. The stalk consists of three joined S2 subunits each capped with an S1 subunit head spreading out in a mushroom-like shape [\[136\]](#)[\[137\]](#)[\[138\]](#)[\[139\]](#). An atomistic model of a full-length trimeric SARS-CoV-2 spike protein with its attached glycans, its C-terminal (stalk) end embedded in the viral envelope, is shown in **Figure 3**.

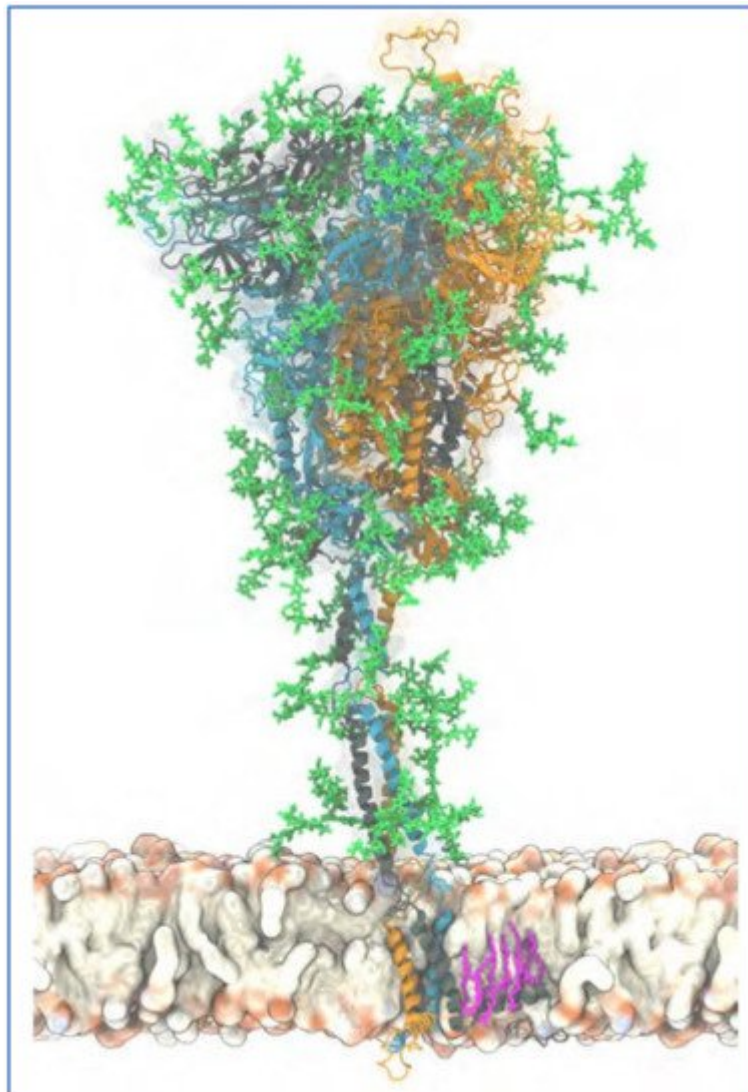


Figure 3. Atomistic model of the full-length trimeric S protein of SARS-CoV-2 shown in cartoon representation. Reproduced from Sikora et al., 2021 [\[140\]](#) (CC-BY 4.0). The three monomeric chains are differentiated by color. Palmitoylated cysteine residues are shown in pink licorice (only one chain shown for clarity), anchored into the viral envelope. Glycans are shown in green licorice representation. A 20 s movie showing a 600 ns atomistic molecular dynamics simulation trajectory of four S proteins embedded in a viral membrane is also provided at this source [\[140\]](#).

A map of the 22 N-linked glycans on each of a spike's three monomers is shown in **Figure 4**. In addition, two O-linked glycosylation sites, S325 and T323, were identified for each spike monomer, both on S1 RBD [86], and both containing SA terminal monosaccharides [141]. Each SARS-CoV-2 virion has a diameter, excluding spikes, of approximately 100 nm, with the number of spikes estimated at up to 65 per virion, these spikes having a length of approximately 20 nm [142][143][144][145].

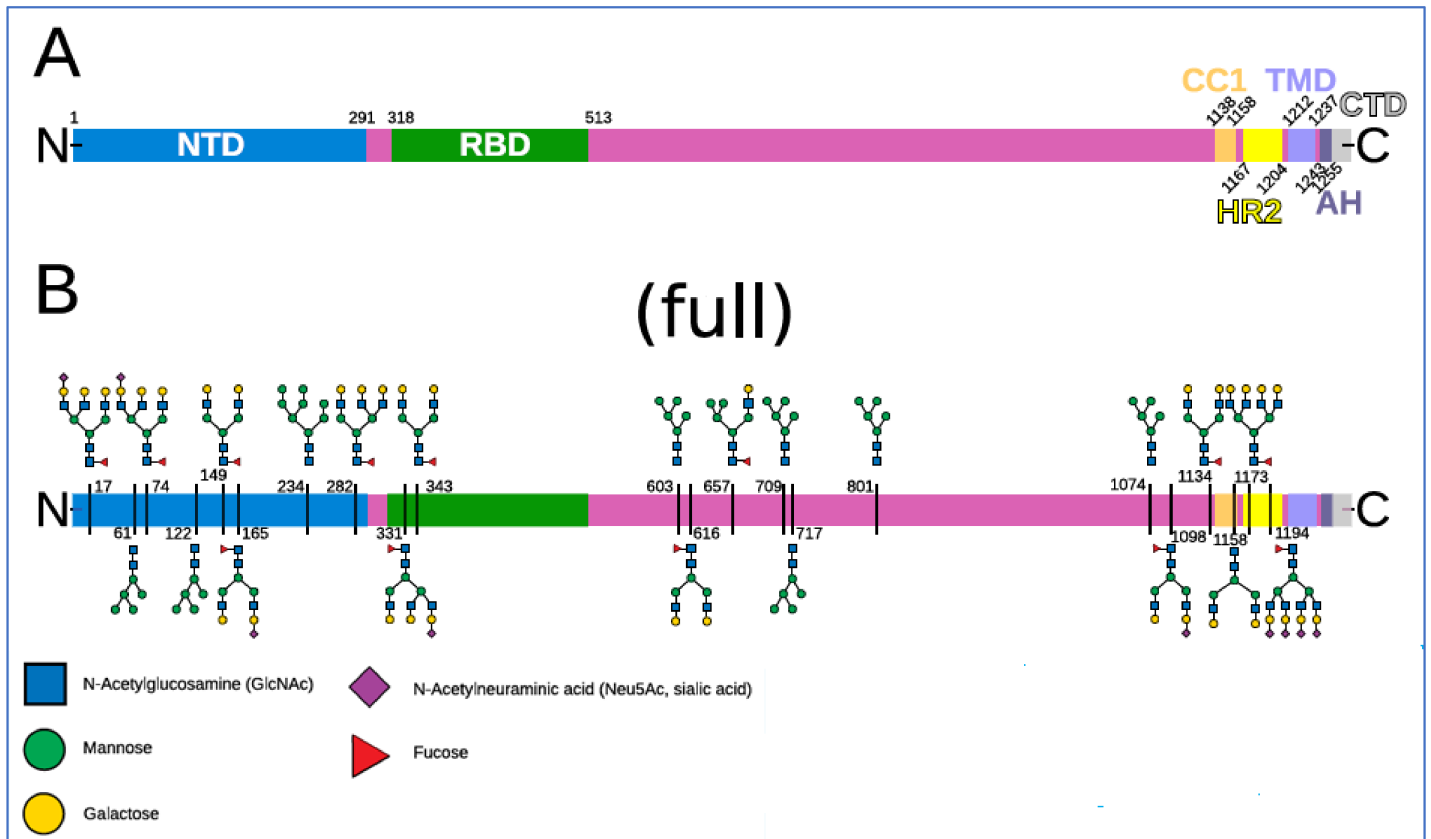


Figure 4. Spike domains and glycosylation. Reproduced from Sikora et al., 2021 [140] (CC-BY 4.0). **(A)** Domains of S (SARS-CoV-2 spike protein). **(B)** Glycosylation pattern of S. Sequons are indicated with the respective glycans in a schematic representation for a fully glycosylated system (“full”). A key to the monosaccharides is shown at the bottom.

The NTD on SARS-CoV-2 spike protein S1, at its N-terminal end, is a focal region for the spike's glycans—eight of the spike's 22 N-glycosylation sites are located there [84][85][86]. The NTD is accordingly the typical point of initial viral attachments to glycoconjugate binding sites on host cells [44][81][82][83][84][85][86][87]. After initial attachment, viral fusion to a host cell begins with linkage of the spike's receptor-binding domain (RBD), situated just below NTD on spike S1, to an ACE2 receptor on the host cell membrane. The S2 stalk then becomes engaged and viral replication proceeds [47][138][146]. The RBD, one on each of a spike's three monomers, constantly switches between open (“up”) and closed (“down”) configurations, the former enabling both ACE2 binding and immune surveillance, the latter blocking both of those functions [136][147].

Researchers' focus now shifts to specifics of virally-mediated clumping of RBCs, notwithstanding the importance of inflammatory processes and endothelial damage in triggering and exacerbating the morbidities of COVID-19, especially in its critical phase. Additionally, platelets, the second most copious blood component [147], serve a pathogen clearance role like that of RBCs [148][149][150], and like RBCs have abundant CD147 and SA surface molecules [151][152][153][154][155][156][157][158]. Platelets can adhere to viruses, RBCs and endothelial cells, especially under inflammatory conditions [16][22][149], and are often enmeshed in clumps that develop in severe malaria between infected and healthy RBCs [159][160][161][162]. Virally induced clumping of RBCs, however, is of particular interest for these reasons. First, as noted above, this clumping alone could limit the efficiency of blood oxygenation in the pulmonary capillaries. Second, such clump formation is directly testable both by examination of the blood of COVID-19 patients and by mixing spike protein with RBCs in vitro. Third, as will be detailed, if such virally induced RBC clumping is confirmed, an existing drug that has been found in silico to bind to glycan sites on both spike protein and host cells can be tested in vitro and clinically for inhibition of virally mediated RBC clumping, in conjunction with an anti-COVID-19 therapeutic benefit.

Of the 22 N-linked glycosylation sites at each of the three monomers of SARS-CoV-2 spike protein, eight are located on NTD as noted above, two on RBD, three others elsewhere on S1, and the other nine on S2 [84][85][86][87]. N1194 is the closest N-glycosylation site from the C-terminal domain, the end of the spike attached to the virion. In different studies, glycans have been identified as populating between 17 and 21 of these 22 N-glycosylation sites [86][87][163][164]. One study found that ten of these 22 sites have terminal SA moieties, in particular of α 5-*N*-acetylneuraminic acid (Neu5Ac), the predominant type of SA found in human cells [25][30]. The terminal monosaccharides on SARS-CoV-2 spike N-glycans other than SA are galactose, mannose, fucose, *N*-acetylglucosamine (GlcNAc) and/or *N*-acetylgalactosamine (GalNAc) [84][87]. As noted above, two SA-tipped O-linked glycans sites have been identified as well, both on S1 RBD [86][141]. Spike protein S1 at its NTD domain was found to bind strongly, in particular to Neu5Ac [94], the type of SA at SARS-CoV-2 N-glycosylation sites and predominant in human cells.

GPA, the major sialoglycoprotein in human RBCs, is of central interest in the attachment of SARS-CoV-2 to RBCs, as observed in vitro [35] and on RBCs of COVID-19 patients [36] as noted above. GPA populates human RBCs at approximately one million molecules per cell and contains most of the SA (of type Neu5Ac) on them [31][33][74][165][166]. GPA molecules have the shapes of strands that are anchored approximately 14 nm apart on the RBC plasma membrane, each extending outwards 5 nm [75]. GPA constitutes the bulk of the RBC's sialoglycoprotein coating, thus determining its 5 nm thickness [75][167][168], and accounts for most of its negative charge [31][169]. Electrostatic repulsion imposes a minimum distance of approximately 8 nm between the outer boundaries of those sialoglycoprotein coatings of adjoining RBCs in a static suspension, but a smaller separation can be achieved when additional forces are pushing these RBCs together [168][170]. SA in its predominant human form, Neu5Ac, is the most common terminal residue of GPA, with its other terminal monosaccharides matching those on SARS-CoV-2 spike N-glycans as noted above: galactose, mannose, fucose, *N*-acetylglucosamine (GlcNAc) and *N*-acetylgalactosamine (GalNAc) [74][75][166]. A representation of a portion of an RBC membrane with strands of GPA and with other glycoproteins interspersed is shown in **Figure 5**.

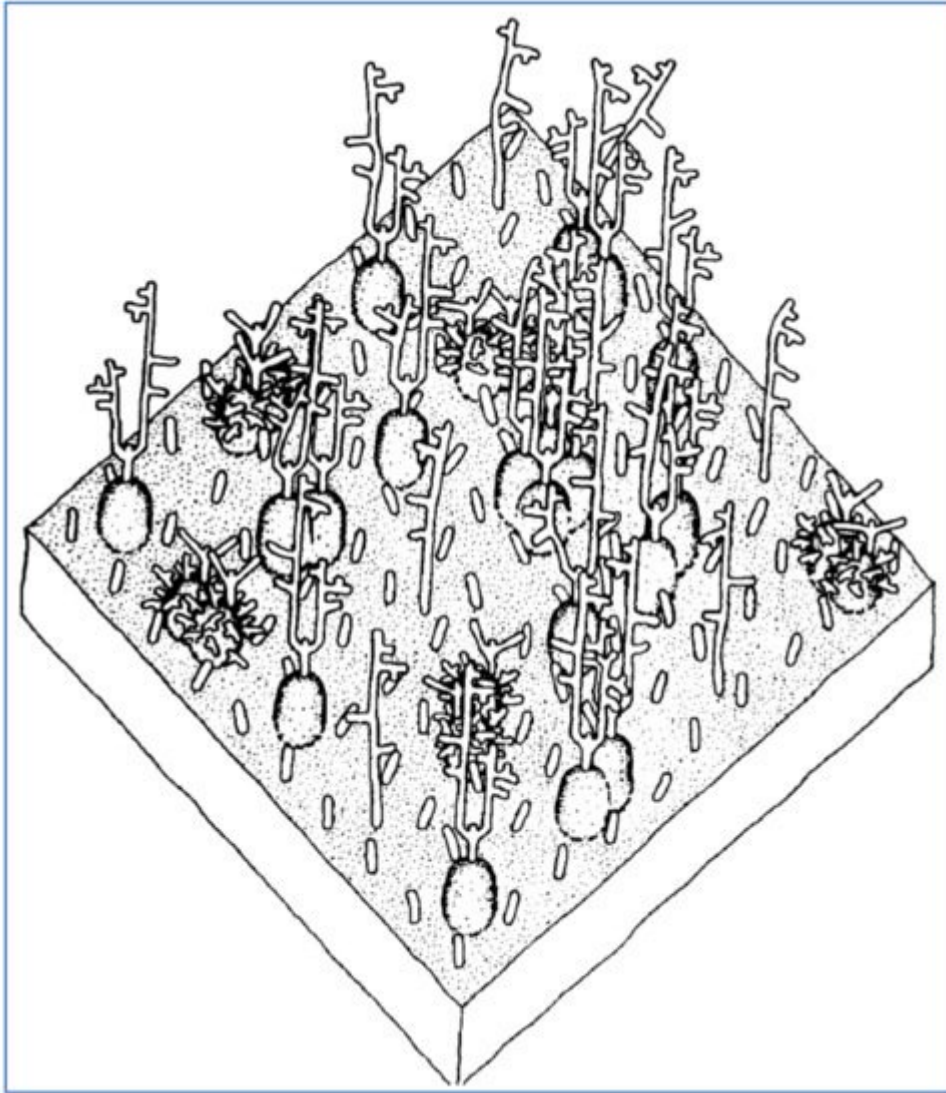


Figure 5. A representation of a 350×350 Angstrom area of the RBC surface depicting its sialoglycoprotein coating, consisting of GPA molecules, extending approximately 5 nm from the RBC cell membrane, plus other smaller glycoprotein molecules interspersed. Reproduced with permission from Elsevier (Viitala, 1985 [\[75\]](#)).

References

1. Valyaeva, A.A.; Zharikova, A.A.; Kasianov, A.S.; Vassetzky, Y.S.; Sheval, E.V. Expression of SARS-CoV-2 entry factors in lung epithelial stem cells and its potential implications for COVID-19. *Sci. Rep.* 2020, 10, 17772.
2. Li, H.; Liu, Z.; Ge, J. Scientific research progress of COVID-19/SARS-CoV-2 in the first five months. *J. Cell. Mol. Med.* 2020, 24, 6558–6570.
3. Zhou, F.; Yu, T.; Du, R.; Fan, G.; Liu, Y.; Liu, Z.; Xiang, J.; Wang, Y.; Song, B.; Gu, X.; et al. Clinical course and risk factors for mortality of adult inpatients with COVID-19 in Wuhan, China: A retrospective cohort study. *Lancet* 2020, 395, 1054–1062.

4. Couzin-Frankel, J. The mystery of the pandemic's 'happy hypoxia'. *Science* 2020, 368, 455–456.
5. Rapkiewicz, A.V.; Mai, X.; Carsons, S.E.; Pittaluga, S.; Kleiner, D.E.; Berger, J.S.; Thomas, S.; Adler, N.M.; Charytan, D.M.; Gasmi, B.; et al. Megakaryocytes and platelet-fibrin thrombi characterize multi-organ thrombosis at autopsy in COVID-19: A case series. *EClinicalMedicine* 2020, 24, 100434.
6. Negri, E.M.; Piloto, B.M.; Morinaga, L.K.; Jardim, C.V.P.; Lamy, S.A.E.-D.; Ferreira, M.A.; D'Amico, E.A.; Deheinzelin, D. Heparin Therapy Improving Hypoxia in COVID-19 Patients—A Case Series. *Front. Physiol.* 2020, 11, 1341.
7. Lodigiani, C.; Lapichino, G.; Carenzo, L.; Cecconi, M.; Ferrazzi, P.; Sebastian, T.; Kucher, N.; Studt, J.D.; Sacco, C.; Alexia, B.; et al. Venous and arterial thromboembolic complications in COVID-19 patients admitted to an academic hospital in Milan, Italy. *Thromb Res.* 2020, 191, 9–14.
8. Price, L.C.; McCabe, C.; Garfield, B.; Wort, S.J. Thrombosis and COVID-19 pneumonia: The clot thickens! *Eur. Respir. J.* 2020, 56, 2001608.
9. Helms, J.; Tacquard, C.; Severac, F.; Leonard-Lorant, I.; Ohana, M.; Delabranche, X.; Merdji, H.; Clere-Jehl, R.; Schenck, M.; Fagot Gandet, F.; et al. High risk of thrombosis in patients with severe SARS-CoV-2 infection: A multicenter prospective cohort study. *Intensive Care Med.* 2020, 46, 1089–1098.
10. Huertas, A.; Montani, D.; Savale, L.; Pichon, J.; Tu, L.; Parent, F.; Guignabert, C.; Humbert, M. Endothelial cell dysfunction: A major player in SARS-CoV-2 infection (COVID-19)? *Eur. Respir. J.* 2020, 56.
11. Sardu, C.; Gambardella, J.; Morelli, M.B.; Wang, X.; Marfella, R.; Santulli, G. Hypertension, thrombosis, kidney failure, and diabetes: Is COVID-19 an endothelial disease? A comprehensive evaluation of clinical and basic evidence. *J. Clin. Med.* 2020, 9, 1417.
12. Jung, F.; Krüger-Genge, A.; Franke, R.P.; Hufert, F.; Küpper, J.H. COVID-19 and the endothelium. *Clin. Hemorheol. Microcirc.* 2020, 75, 7–11.
13. Gupta, A.; Madhavan, M.V.; Sehgal, K.; Nair, N.; Mahajan, S.; Sehrawat, T.S.; Bikdeli, B.; Ahluwalia, N.; Ausiello, J.C.; Wan, E.Y.; et al. Extrapulmonary manifestations of COVID-19. *Nat. Med.* 2020, 26, 1017–1032.
14. Bikdeli, B.; Madhavan, M.V.; Jimenez, D.; Chuich, T.; Dreyfus, I.; Driggin, E.; Nigoghossian, C.; Ageno, W.; Madjid, M.; Guo, Y.; et al. COVID-19 and thrombotic or thromboembolic disease: Implications for prevention, antithrombotic therapy, and follow-up: JACC state-of-the-art review. *J. Am. Coll. Cardiol.* 2020, 75, 2950–2973.
15. Libby, P.; Lüscher, T. COVID-19 is, in the end, an endothelial disease. *Eur. Heart J.* 2020, 41, 3038–3044.

16. Becker, R.C. COVID-19 update: Covid-19-associated coagulopathy. *J. Thromb Thrombolysis* 2020, 50, 54–67.
17. Mondal, R.; Lahiri, D.; Deb, S.; Bandyopadhyay, D.; Shome, G.; Sarkar, S.; Paria, S.R.; Thakurta, T.G.; Singla, P.; Biswas, S.C. COVID-19: Are we dealing with a multisystem vasculopathy in disguise of a viral infection? *J. Thromb Thrombolysis* 2020, 50, 567–579.
18. Magro, C.; Mulvey, J.J.; Berlin, D.; Nuovo, G.; Salvatore, S.; Harp, J.; Baxter-Stoltzfus, A.; Laurence, J. Complement associated microvascular injury and thrombosis in the pathogenesis of severe COVID-19 infection: A report of five cases. *Transl. Res.* 2020, 220, 1–13.
19. Menter, T.; Haslbauer, J.D.; Nienhold, R.; Savic, S.; Hopfer, H.; Deigendesch, N.; Frank, S.; Turek, D.; Willi, N.; Pargger, H.; et al. Postmortem examination of COVID-19 patients reveals diffuse alveolar damage with severe capillary congestion and variegated findings in lungs and other organs suggesting vascular dysfunction. *Histopathology* 2020, 77, 198–209.
20. Gattinoni, L.; Coppola, S.; Cressoni, M.; Busana, M.; Rossi, S.; Chiumello, D. COVID-19 does not lead to a “typical” acute respiratory distress syndrome. *Am. J. Respir. Crit. Care Med.* 2020, 201, 1299–1300.
21. Marini, J.J.; Gattinoni, L. Management of COVID-19 respiratory distress. *JAMA* 2020, 323, 2329–2330.
22. Scheim, D.E. From Cold to Killer: How SARS-CoV-2 Evolved without Hemagglutinin Esterase to Agglutinate, then Clot Blood Cells in Pulmonary and Systemic Microvasculature. Available online: <http://ssrn.com/abstract=3706347> (accessed on 24 November 2021).
23. Bourgonje, A.R.; Abdulle, A.E.; Timens, W.; Hillebrands, J.L.; Navis, G.J.; Gordijn, S.J.; Bolling, M.C.; Dijkstra, G.; Voors, A.A.; Osterhaus, A.; et al. Angiotensin-converting enzyme-2 (ACE2), SARS-CoV-2 and pathophysiology of coronavirus disease 2019 (COVID-19). *J. Pathol.* 2020, 25, 228–248.
24. Wang, Q.; Zhang, Y.; Wu, L.; Niu, S.; Song, C.; Zhang, Z.; Lu, G.; Qiao, C.; Hu, Y.; Yuen, K.-Y.; et al. Structural and functional basis of SARS-CoV-2 entry by using human ACE2. *Cell* 2020, 181, 894–904.e899.
25. Ströh, L.J.; Stehle, T. Glycan engagement by viruses: Receptor switches and specificity. *Annu Rev. Virol* 2014, 1, 285–306.
26. Milanetti, E.; Miotto, M.; Di Rienzo, L.; Nagaraj, M.; Monti, M.; Golbek, T.W.; Gosti, G.; Roeters, S.J.; Weidner, T.; Otzen, D.E.; et al. In-Silico Evidence for a Two Receptor Based Strategy of SARS-CoV-2. *Front Mol Biosci* 2021, 8, 690655.
27. Morniroli, D.; Gianni, M.L.; Consales, A.; Pietrasanta, C.; Mosca, F. Human sialome and coronavirus disease-2019 (COVID-19) pandemic: An understated correlation? *Front. Immunol.* 2020, 11, 1480.

28. Fantini, J.; Di Scala, C.; Chahinian, H.; Yahi, N. Structural and molecular modelling studies reveal a new mechanism of action of chloroquine and hydroxychloroquine against SARS-CoV-2 infection. *Int. J. Antimicrob. Agents* 2020, 55, 105960.
29. Roe, K. High COVID-19 virus replication rates, the creation of antigen–antibody immune complexes and indirect haemagglutination resulting in thrombosis. *Transbound. Emerg. Dis.* 2020, 67, 1418–1421.
30. Koehler, M.; Delguste, M.; Sieben, C.; Gillet, L.; Alsteens, D. Initial step of virus entry: Virion binding to cell-surface glycans. *Annu. Rev. Virol.* 2020, 7, 143–165.
31. Baum, J.; Ward, R.H.; Conway, D.J. Natural selection on the erythrocyte surface. *Mol. Biol. Evol.* 2002, 19, 223–229.
32. Storry, J.R. Review: The function of blood group-specific RBC membrane components. *Immunohematology* 2004, 20, 206–216.
33. Levine, S.; Levine, M.; Sharp, K.A.; Brooks, D.E. Theory of the electrokinetic behavior of human erythrocytes. *Biophys. J.* 1983, 42, 127–135.
34. Bai, Y.; Huang, W.; Ma, L.T.; Jiang, J.L.; Chen, Z.N. Importance of N-glycosylation on CD147 for its biological functions. *Int. J. Mol. Sci.* 2014, 15, 6356–6377.
35. Modrof, J.; Kerschbaum, A.; Farcet, M.R.; Niemeyer, D.; Corman, V.M.; Kreil, T.R. SARS-CoV-2 and the safety margins of cell-based biological medicinal products. *Biologicals* 2020, 68, 122–124.
36. Lam, L.M.; Murphy, S.J.; Kuri-Cervantes, L.; Weisman, A.R.; Ittner, C.A.G.; Reilly, J.P.; Pampena, M.B.; Betts, M.R.; Wherry, E.J.; Song, W.-C.; et al. Erythrocytes reveal complement activation in patients with COVID-19. *medRxiv* 2020, 05.20.20104398.
37. Howe, C.; Lee, L.T. Virus-erythrocyte interactions. In *Advances in Virus Research*; Smith, K.M., Lauffer, M.A., Bang, F.B., Eds.; Academic Press: New York, NY, USA, 1972; Volume 17, pp. 1–50.
38. Matrosovich, M.; Herrler, G.; Klenk, H.D. Sialic acid receptors of viruses. In *SialoGlyco Chemistry and Biology II: Tools and Techniques to Identify and Capture Sialoglycans*; Gerardy-Schahn, R., Delannoy, P., von Itzstein, M., Eds.; Springer International Publishing: New York, NY, USA, 2015; pp. 1–28.
39. Kapikian, A.Z.; James, H.D., Jr.; Kelly, S.J.; King, L.M.; Vaughn, A.L.; Chanock, R.M. Hemadsorption by coronavirus strain OC43. *Proc. Soc. Exp. Biol. Med.* 1972, 139, 179–186.
40. Agafonov, A.P.; Gus'kov, A.A.; Ternovoi, V.A.; Ryabchikova, E.I.; Durymanov, A.G.; Vinogradov, I.V.; Maksimov, N.L.; Ignat'ev, G.M.; Nechaeva, E.A.; Netesov, S.V. Primary characterization of SARS coronavirus strain Frankfurt 1. *Dokl. Biol. Sci.* 2004, 394, 58–60.

41. Vlasak, R.; Luytjes, W.; Spaan, W.; Palese, P. Human and bovine coronaviruses recognize sialic acid-containing receptors similar to those of influenza C viruses. *Proc. Natl. Acad. Sci. USA* 1988, 85, 4526–4529.
42. Storz, J.; Zhang, X.M.; Rott, R. Comparison of hemagglutinating, receptor-destroying, and acetylcholinesterase activities of avirulent and virulent bovine coronavirus strains. *Arch. Virol.* 1992, 125, 193–204.
43. Brian, D.A.; Hogue, B.G.; Kienzle, T.E. The coronavirus hemagglutinin esterase glycoprotein. In *The Coronaviridae. The Viruses*; Siddell, S.G., Ed.; Springer: Boston, MA, USA, 1995.
44. Qing, E.; Hantak, M.; Perlman, S.; Gallagher, T. Distinct Roles for sialoside and protein receptors in coronavirus infection. *mBio* 2020, 11, e02764–e02819.
45. Schultze, B.; Cavanagh, D.; Herrler, G. Neuraminidase treatment of avian infectious bronchitis coronavirus reveals a hemagglutinating activity that is dependent on sialic acid-containing receptors on erythrocytes. *Virology* 1992, 189, 792–794.
46. Schultze, B.; Enjuanes, L.; Herrler, G. Analysis of the sialic acid-binding activity of transmissible gastroenteritis virus. In *Corona- and Related Viruses: Current Concepts in Molecular Biology and Pathogenesis*; Talbot, P.J., Levy, G.A., Eds.; Springer: Boston, MA, USA, 1995; pp. 367–370.
47. Hulswit, R.J.G.; de Haan, C.A.M.; Bosch, B.J. Chapter two—Coronavirus spike protein and tropism changes. In *Advances in Virus Research*; Ziebuhr, J., Ed.; Academic Press: New York, NY, USA, 2016; Volume 96, pp. 29–57.
48. Li, W.; Hulswit, R.J.G.; Widjaja, I.; Raj, V.S.; McBride, R.; Peng, W.; Widagdo, W.; Tortorici, M.A.; van Dieren, B.; Lang, Y.; et al. Identification of sialic acid-binding function for the Middle East respiratory syndrome coronavirus spike glycoprotein. *Proc. Natl. Acad. Sci. USA* 2017, 114, E8508–E8517.
49. Hirst, G.K. The agglutination of red cells by allantoic fluid of chick embryos infected with influenza virus. *Science* 1941, 94, 22–23.
50. Hirst, G.K. Adsorption of influenza hemagglutinins and virus by red blood cells. *J. Exp. Med.* 1942, 76, 195–209.
51. McClelland, L.; Hare, R. The adsorption of influenza virus by red cells and a new in vitro method of measuring antibodies for influenza virus. *Can. Public Health J.* 1941, 32, 530–538.
52. Salk, J.E. A Simplified procedure for titrating hemagglutinating capacity of influenza-virus and the corresponding antibody. *J. Immunol.* 1944, 49, 87–98.
53. Salk, J.E. A plastic plate for use in tests involving virus hemagglutination and other similar reactions. *Science* 1948, 108, 749.

54. Hierholzer, J.C.; Suggs, M.T.; Hall, E.C. Standardized viral hemagglutination and hemagglutination-inhibition tests. II. Description and statistical evaluation. *Appl Microbiol* 1969, 18, 824–833.
55. Defang, G.N.; Martin, N.J.; Burgess, T.H.; Millar, E.V.; Pecenka, L.A.; Danko, J.R.; Arnold, J.C.; Kochel, T.J.; Luke, T.C. Comparative analysis of hemagglutination inhibition titers generated using temporally matched serum and plasma samples. *PLoS ONE* 2012, 7, e48229.
56. Nguyen, M.; Fries, K.; Khoury, R.; Zheng, L.; Hu, B.; Hildreth, S.W.; Parkhill, R.; Warren, W. Automated imaging and analysis of the hemagglutination inhibition assay. *J. Lab. Autom.* 2015, 21, 287–296.
57. Killian, M.L. Hemagglutination assay for influenza virus. In *Animal Influenza Virus*; Spackman, E., Ed.; Springer: New York, NY, USA, 2014; pp. 3–9.
58. Barrett, T.; Inglis, S. Growth, purification and titration of influenza viruses. In *Virology: A Practical Approach*; Mahy, Ed.; Oxford IRL Press Ltd.: Oxford, UK, 1985; pp. 119–150.
59. Ryu, W.-S. Chapter 4—Diagnosis and methods. In *Molecular Virology of Human Pathogenic Viruses*; Ryu, W.-S., Ed.; Academic Press: Boston, MA, USA, 2017; pp. 47–62.
60. Pedersen, J.C. Hemagglutination-inhibition assay for influenza virus subtype identification and the detection and quantitation of serum antibodies to influenza Virus. In *Animal Influenza Virus*; Spackman, E., Ed.; Springer: New York, NY, USA, 2014; pp. 11–25.
61. Bakkers, M.J.G.; Lang, Y.; Feitsma, L.J.; Hulswit, R.J.G.; de Poot, S.A.H.; van Vliet, A.L.W.; Margine, I.; de Groot-Mijnes, J.D.F.; van Kuppeveld, F.J.M.; Langereis, M.A.; et al. Betacoronavirus adaptation to humans involved progressive loss of hemagglutinin-esterase lectin activity. *Cell Host Microbe* 2017, 21, 356–366.
62. Hulswit, R.J.G.; Lang, Y.; Bakkers, M.J.G.; Li, W.; Li, Z.; Schouten, A.; Ophorst, B.; van Kuppeveld, F.J.M.; Boons, G.J.; Bosch, B.J.; et al. Human coronaviruses OC43 and HKU1 bind to 9-O-acetylated sialic acids via a conserved receptor-binding site in spike protein domain A. *Proc. Natl. Acad. Sci. USA* 2019, 116, 2681–2690.
63. Neu, U.; Bauer, J.; Stehle, T. Viruses and sialic acids: Rules of engagement. *Curr. Opin. Struct. Biol.* 2011, 21, 610–618.
64. Huang, X.; Dong, W.; Milewska, A.; Golda, A.; Qi, Y.; Zhu, Q.K.; Marasco, W.A.; Baric, R.S.; Sims, A.C.; Pyrc, K.; et al. Human Coronavirus HKU1 spike protein uses o-acetylated sialic acid as an attachment receptor determinant and employs hemagglutinin-esterase protein as a receptor-destroying enzyme. *J. Virol.* 2015, 89, 7202–7213.
65. Dai, X.; Zhang, X.; Ostrikov, K.; Abrahamyan, L. Host receptors: The key to establishing cells with broad viral tropism for vaccine production. *Crit. Rev. Microbiol.* 2020, 46, 147–168.

66. Newton, R.; Delguste, M.; Koehler, M.; Dumitru, A.C.; Laskowski, P.R.; Müller, D.J.; Alsteens, D. Combining confocal and atomic force microscopy to quantify single-virus binding to mammalian cell surfaces. *Nat. Protoc.* 2017, 12, 2275–2292.
67. Park, Y.-J.; Walls, A.C.; Wang, Z.; Sauer, M.M.; Li, W.; Tortorici, M.A.; Bosch, B.-J.; DiMaio, F.; Veesler, D. Structures of MERS-CoV spike glycoprotein in complex with sialoside attachment receptors. *Nat. Struct. Mol. Biol.* 2019, 26, 1151–1157.
68. Sieben, C.; Kappel, C.; Zhu, R.; Wozniak, A.; Rankl, C.; Hinterdorfer, P.; Grubmüller, H.; Herrmann, A. Influenza virus binds its host cell using multiple dynamic interactions. *Proc. Natl. Acad. Sci. USA* 2012, 109, 13626–13631.
69. Tiralongo, J. Chapter 29—Sialic acid-specific microbial lectins. In *Microbial Glycobiology*; Holst, O., Brennan, P.J., Itzstein, M.V., Moran, A.P., Eds.; Academic Press: San Diego, CA, USA, 2010; pp. 585–598.
70. Wielgat, P.; Rogowski, K.; Godlewska, K.; Car, H. Coronaviruses: Is Sialic acid a gate to the eye of cytokine storm? From the entry to the effects. *Cells* 2020, 9, 1963.
71. Nelson, D.S. Immune adherence. In *Advances in Immunology*; Dixon, F.J., Humphrey, J.H., Eds.; Academic Press: Cambridge, MA, USA, 1963; Volume 3, pp. 131–180.
72. Anderson, H.L.; Brodsky, I.E.; Mangalmurti, N.S. The evolving erythrocyte: Red blood cells as modulators of innate immunity. *J. Immunol.* 2018, 201, 1343–1351.
73. Varki, A.; Gagneux, P. Multifarious roles of sialic acids in immunity. *Ann. N. Y. Acad. Sci.* 2012, 1253, 16–36.
74. Aoki, T. A comprehensive review of our current understanding of red blood cell (RBC) glycoproteins. *Membranes* 2017, 7, 56.
75. Viitala, J.; Järnefelt, J. The red cell surface revisited. *Trends Biochem. Sci.* 1985, 10, 392–395.
76. De Back, D.Z.; Kostova, E.; Klei, T.; Beuger, B.; van Zwieten, R.; Kuijpers, T.; Juffermans, N.; van den Berg, T.; Korte, D.; van Kraaij, M.; et al. RBC Adhesive Capacity Is Essential for Efficient ‘Immune Adherence Clearance’ and Provide a Generic Target to Deplete Pathogens from Septic Patients. *Blood* 2016, 128, 1031.
77. Nelson, R.A. The Immune-Adherence Phenomenon: An Immunologically Specific Reaction Between Microorganisms and Erythrocytes Leading to Enhanced Phagocytosis. *Science* 1953, 118, 733–737.
78. Nelson, R.A., Jr. The immune-adherence phenomenon; a hypothetical role of erythrocytes in defence against bacteria and viruses. *Proc. R Soc. Med.* 1956, 49, 55–58.
79. de Groot, R.J.; Baker, S.C.; Baric, R.; Enjuanes, L. Family—Coronaviridae. In *Virus Taxonomy: Ninth Report of the International Committee on Taxonomy of Viruses*; King, A.M.Q., Adams, M.J.,

- Carstens, E.B., Lefkowitz, E.J., Eds.; Elsevier: San Diego, CA, USA, 2012; pp. 806–828.
80. Sriwilaijaroen, N.; Suzuki, Y. Sialoglycovirolgy of lectins: Sialyl Glycan binding of enveloped and non-enveloped viruses. In *Lectin Purification and Analysis: Methods and Protocols*; Hirabayashi, J., Ed.; Springer: New York, NY, USA, 2020; pp. 483–545.
81. Lang, Y.; Li, W.; Li, Z.; Koerhuis, D.; van den Burg, A.C.S.; Rozemuller, E.; Bosch, B.-J.; van Kuppeveld, F.J.M.; Boons, G.-J.; Huizinga, E.G.; et al. Coronavirus hemagglutinin-esterase and spike proteins coevolve for functional balance and optimal virion avidity. *Proc. Natl. Acad. Sci. USA* 2020, *117*, 25759–25770.
82. Belouzard, S.; Millet, J.K.; Licitra, B.N.; Whittaker, G.R. Mechanisms of coronavirus cell entry mediated by the viral spike protein. *Viruses* 2012, *4*, 1011–1033.
83. Awasthi, M.; Gulati, S.; Sarkar, D.; Tiwari, S.; Kateriya, S.; Ranjan, P.; Verma, S.K. The Sialoside-Binding Pocket of SARS-CoV-2 Spike Glycoprotein Structurally Resembles MERS-CoV. *Viruses* 2020, *12*, 909.
84. Chen, W.; Hui, Z.; Ren, X.; Luo, Y.; Shu, J.; Yu, H.; Li, Z. The N-glycosylation sites and Glycan-binding ability of S-protein in SARS-CoV-2 Coronavirus. *bioRxiv* 2020, 12.01.406025.
85. Guo, W.; Lakshminarayanan, H.; Rodriguez-Palacios, A.; Salata, R.A.; Xu, K.; Draz, M.S. Glycan Nanostructures of Human Coronaviruses. *Int. J. Nanomed.* 2021, *16*, 4813–4830.
86. Shajahan, A.; Supekar, N.T.; Gleinich, A.S.; Azadi, P. Deducing the N- and O-glycosylation profile of the spike protein of novel coronavirus SARS-CoV-2. *Glycobiology* 2020, *30*, 981–988.
87. Gao, C.; Zeng, J.; Jia, N.; Stavenhagen, K.; Matsumoto, Y.; Zhang, H.; Li, J.; Hume, A.J.; Mühlberger, E.; van Die, I.; et al. SARS-CoV-2 Spike Protein Interacts with Multiple Innate Immune Receptors. *bioRxiv* 2020, 07.29.227462.
88. Chan, J.F.-W.; Kok, K.-H.; Zhu, Z.; Chu, H.; To, K.K.-W.; Yuan, S.; Yuen, K.-Y. Genomic characterization of the 2019 novel human-pathogenic coronavirus isolated from a patient with atypical pneumonia after visiting Wuhan. *Emerg. Microbes Infect.* 2020, *9*, 221–236.
89. Chen, Y.; Liu, Q.; Guo, D. Emerging coronaviruses: Genome structure, replication, and pathogenesis. *J. Med. Virol.* 2020, *92*, 418–423.
90. Zaki, A.M.; van Boheemen, S.; Bestebroer, T.M.; Osterhaus, A.D.; Fouchier, R.A. Isolation of a novel coronavirus from a man with pneumonia in Saudi Arabia. *N. Engl. J. Med.* 2012, *367*, 1814–1820.
91. Kumar, S.; Nyodu, R.; Maurya, V.K.; Saxena, S.K. Morphology, Genome Organization, Replication, and Pathogenesis of Severe Acute Respiratory Syndrome Coronavirus 2 (SARS-CoV-2). In *Coronavirus Disease 2019 (COVID-19): Epidemiology, Pathogenesis, Diagnosis, and Therapeutics*; Saxena, S.K., Ed.; Springer: Singapore, 2020; pp. 23–31.

92. Yoshimoto, F.K. The Proteins of Severe Acute Respiratory Syndrome Coronavirus-2 (SARS CoV-2 or n-COV19), the Cause of COVID-19. *Protein J.* 2020, 39, 198–216.
93. Bakkers, M.J.G.; Zeng, Q.; Feitsma, L.J.; Hulswit, R.J.G.; Li, Z.; Westerbeke, A.; van Kuppeveld, F.J.M.; Boons, G.-J.; Langereis, M.A.; Huizinga, E.G.; et al. Coronavirus receptor switch explained from the stereochemistry of protein–carbohydrate interactions and a single mutation. *Proc. Natl. Acad. Sci. USA* 2016, 113, E3111–E3119.
94. Baker, A.N.; Richards, S.-J.; Guy, C.S.; Congdon, T.R.; Hasan, M.; Zwetsloot, A.J.; Gallo, A.; Lewandowski, J.R.; Stansfeld, P.J.; Straube, A.; et al. The SARS-COV-2 Spike Protein Binds Sialic Acids and Enables Rapid Detection in a Lateral Flow Point of Care Diagnostic Device. *ACS Cent. Sci.* 2020, 6, 2046–2052.
95. Collins, B.E.; Paulson, J.C. Cell surface biology mediated by low affinity multivalent protein–glycan interactions. *Curr. Opin. Chem. Biol.* 2004, 8, 617–625.
96. Cohen, M.; Varki, A. Chapter Three—Modulation of Glycan Recognition by Clustered Saccharide Patches. In *International Review of Cell and Molecular Biology*; Jeon, K.W., Ed.; Academic Press: Cambridge, MA, USA, 2014; Volume 308, pp. 75–125.
97. Xiong, X.; Coombs, P.J.; Martin, S.R.; Liu, J.; Xiao, H.; McCauley, J.W.; Locher, K.; Walker, P.A.; Collins, P.J.; Kawaoka, Y.; et al. Receptor binding by a ferret-transmissible H5 avian influenza virus. *Nature* 2013, 497, 392–396.
98. Xu, H.; Shaw, D.E. A simple model of multivalent adhesion and its application to influenza infection. *Biophys. J.* 2016, 110, 218–233.
99. Sauter, N.K.; Hanson, J.E.; Glick, G.D.; Brown, J.H.; Crowther, R.L.; Park, S.J.; Skehel, J.J.; Wiley, D.C. Binding of influenza virus hemagglutinin to analogs of its cell-surface receptor, sialic acid: Analysis by proton nuclear magnetic resonance spectroscopy and X-ray crystallography. *Biochemistry* 1992, 31, 9609–9621.
100. Mitnaul, L.J.; Matrosovich, M.N.; Castrucci, M.R.; Tuzikov, A.B.; Bovin, N.V.; Kobasa, D.; Kawaoka, Y. Balanced Hemagglutinin and Neuraminidase Activities Are Critical for Efficient Replication of Influenza A Virus. *J. Virol.* 2000, 74, 6015–6020.
101. Pourrajab, F.; Zare-Khormizi, M.R.; Sheikhha, M.H. Molecular basis for pathogenicity of human coronaviruses. *Infect. Drug Resist.* 2020, 13, 2385–2405.
102. Radzikowska, U.; Ding, M.; Tan, G.; Zhakparov, D.; Peng, Y.; Wawrzyniak, P.; Wang, M.; Li, S.; Morita, H.; Altunbulakli, C.; et al. Distribution of ACE2, CD147, CD26, and other SARS-CoV-2 associated molecules in tissues and immune cells in health and in asthma, COPD, obesity, hypertension, and COVID-19 risk factors. *Allergy* 2020, 75, 2829–2845.
103. Silva-Filho, J.C.; Melo, C.G.F.d.; Oliveira, J.L.d. The influence of ABO blood groups on COVID-19 susceptibility and severity: A molecular hypothesis based on carbohydrate-carbohydrate

- interactions. *Med. Hypotheses* 2020, 144, 110155.
104. Wang, K.; Chen, W.; Zhang, Z.; Deng, Y.; Lian, J.-Q.; Du, P.; Wei, D.; Zhang, Y.; Sun, X.-X.; Gong, L.; et al. CD147-spike protein is a novel route for SARS-CoV-2 infection to host cells. *Signal. Transduct. Target. Ther.* 2020, 5, 283.
 105. Bian, H.; Zheng, Z.-H.; Wei, D.; Wen, A.; Zhang, Z.; Lian, J.-Q.; Kang, W.-Z.; Hao, C.-Q.; Wang, J.; Xie, R.-H.; et al. Safety and efficacy of meplazumab in healthy volunteers and COVID-19 patients: A randomized phase 1 and an exploratory phase 2 trial. *Signal. Transduct. Target. Ther.* 2021, 6, 194.
 106. Shelokov, A.; Vogel, J.E.; Chi, L. Hemadsorption (Adsorption-Hemagglutination) Test for Viral Agents in Tissue Culture with Special Reference to Influenza. *Proc. Soc. Exp. Biol. Med.* 1958, 97, 802–809.
 107. Gagnetten, S.; Gout, O.; Dubois-Dalcq, M.; Rottier, P.; Rossen, J.; Holmes, K.V. Interaction of mouse hepatitis virus (MHV) spike glycoprotein with receptor glycoprotein MHVR is required for infection with an MHV strain that expresses the hemagglutinin-esterase glycoprotein. *J. Virol.* 1995, 69, 889–895.
 108. Adams, J.H.; Sim, B.K.; Dolan, S.A.; Fang, X.; Kaslow, D.C.; Miller, L.H. A family of erythrocyte binding proteins of malaria parasites. *Proc. Natl. Acad. Sci. USA* 1992, 89, 7085–7089.
 109. Persson, K.E.; McCallum, F.J.; Reiling, L.; Lister, N.A.; Stubbs, J.; Cowman, A.F.; Marsh, K.; Beeson, J.G. Variation in use of erythrocyte invasion pathways by *Plasmodium falciparum* mediates evasion of human inhibitory antibodies. *J. Clin. Invest.* 2008, 118, 342–351.
 110. Crosnier, C.; Bustamante, L.Y.; Bartholdson, S.J.; Bei, A.K.; Theron, M.; Uchikawa, M.; Mboup, S.; Ndir, O.; Kwiatkowski, D.P.; Duraisingh, M.T.; et al. Basigin is a receptor essential for erythrocyte invasion by *Plasmodium falciparum*. *Nature* 2011, 480, 534–537.
 111. Zenonos, Z.A.; Dummler, S.K.; Müller-Sienerth, N.; Chen, J.; Preiser, P.R.; Rayner, J.C.; Wright, G.J. Basigin is a druggable target for host-oriented antimalarial interventions. *J. Exp. Med.* 2015, 212, 1145–1151.
 112. Berzuini, A.; Bianco, C.; Migliorini, A.C.; Maggioni, M.; Valenti, L.; Prati, D. Red blood cell morphology in patients with COVID-19-related anaemia. *Blood Transfus.* 2021, 19, 34–36.
 113. Lakhdari, N.; Tabet, B.; Boudraham, L.; Laoussati, M.; Aissanou, S.; Beddou, L.; Bensalem, S.; Bellik, Y.; Bournine, L.; Fatmi, S.; et al. Red blood cells injuries and hypersegmented neutrophils in COVID-19 peripheral blood film. *medRxiv* 2020, 07.24.20160101.
 114. Melkumyants, A.; Buryachkovskaya, L.; Lomakin, N.; Antonova, O.; Serebruany, V. Mild COVID-19 and impaired blood cell–endothelial crosstalk: Considering long-term use of antithrombotics? *Thromb. Haemost.* 2022, 122, 123–130.

115. Diez-Silva, M.; Dao, M.; Han, J.; Lim, C.-T.; Suresh, S. Shape and Biomechanical Characteristics of Human Red Blood Cells in Health and Disease. *MRS Bull.* 2010, 35, 382–388.
116. Guest, M.M.; Bond, T.P.; Cooper, R.G.; Derrick, J.R. Red Blood Cells: Change in Shape in Capillaries. *Science* 1963, 142, 1319–1321.
117. Shahid, M.; Nunhuck, A. *Physiology*; Elsevier Health Sciences: Philadelphia, PA, USA, 2008; p. 273.
118. Kuchel, P.W.; Shishmarev, D. Accelerating metabolism and transmembrane cation flux by distorting red blood cells. *Sci. Adv.* 2017, 3, EAAO1016.
119. Ocak, I.; Kara, A.; Ince, C. Monitoring microcirculation. *Best Pract. Res. Clin. Anaesthesiol.* 2016, 30, 407–418.
120. Chasis, J.A.; Mohandas, N. Red blood cell glycoporphins. *Blood* 1992, 80, 1869–1879.
121. Barshtein, G.; Wajnblum, D.; Yedgar, S. Kinetics of linear rouleaux formation studied by visual monitoring of red cell dynamic organization. *Biophys. J.* 2000, 78, 2470–2474.
122. Fung, Y.-C. The flow properties of blood. In *Biomechanics: Mechanical Properties of Living Tissues*; Fung, Y.-C., Ed.; Springer New York: New York, NY, USA, 1993; pp. 66–108.
123. Maeda, N.; Seike, M.; Kon, K.; Shiga, T. Erythrocyte Aggregation as a Determinant of Blood Flow: Effect of pH, Temperature and Osmotic Pressure. In *Oxygen Transport to Tissue X*; Mochizuki, M., Honig, C.R., Koyama, T., Goldstick, T.K., Bruley, D.F., Eds.; Springer: New York, NY, USA, 1988; pp. 563–570.
124. Sakariassen, K.S.; Orning, L.; Turitto, V.T. The impact of blood shear rate on arterial thrombus formation. *Future Sci. OA* 2015, 1, FSO30.
125. Ahmetaj-Shala, B.; Vaja, R.; Atanur, S.; George, P.; Kirkby, N.; Mitchell, J. Systemic analysis of putative SARS-CoV-2 entry and processing genes in cardiovascular tissues identifies a positive correlation of BSG with age in endothelial cells. *bioRxiv* 2020, 06.23.165324.
126. Ackermann, M.; Verleden, S.E.; Kuehnel, M.; Haverich, A.; Welte, T.; Laenger, F.; Vanstapel, A.; Werlein, C.; Stark, H.; Tzankov, A.; et al. Pulmonary Vascular Endothelialitis, Thrombosis, and Angiogenesis in Covid-19. *N. Engl. J. Med.* 2020, 383, 120–128.
127. Siddiqi, H.; Libby, P.; Ridker, P. COVID-19 and vascular disease. *EBioMedicine* 2020, 58, 102966.
128. Lee, M.-H.; Perl, D.P.; Nair, G.; Li, W.; Maric, D.; Murray, H.; Dodd, S.J.; Koretsky, A.P.; Watts, J.A.; Cheung, V.; et al. Microvascular Injury in the Brains of Patients with Covid-19. *N. Engl. J. Med.* 2020, 384, 481–483.
129. Colunga Biancatelli, R.M.L.; Solopov, P.A.; Sharlow, E.R.; Lazo, J.S.; Marik, P.E.; Catravas, J.D. The SARS-CoV-2 spike protein subunit S1 induces COVID-19-like acute lung injury in K18-

- hACE2 transgenic mice and barrier dysfunction in human endothelial cells. *Am. J. Physiol. Lung Cell Mol. Physiol.* 2021, 321, L477–L484.
130. Nuovo, G.J.; Magro, C.; Shaffer, T.; Awad, H.; Suster, D.; Mikhail, S.; He, B.; Michaille, J.-J.; Liechty, B.; Tili, E. Endothelial cell damage is the central part of COVID-19 and a mouse model induced by injection of the S1 subunit of the spike protein. *Ann. Diagn. Pathol.* 2021, 51, 151682.
 131. Perico, L.; Morigi, M.; Galbusera, M.; Pezzotta, A.; Gastoldi, S.; Imberti, B.; Ruggenti, P.; Benigni, A.; Remuzzi, G. SARS-CoV-2 Spike Protein 1 Activates Microvascular Endothelial Cells and Complement System Leading to Thrombus Formation. Available online: <https://ssrn.com/abstract=3864027> (accessed on 23 November 2021).
 132. Magro, C.; Mulvey, J.J.; Laurence, J.; Sanders, S.; Crowson, N.; Grossman, M.; Harp, J.; Nuovo, G. The differing pathophysiologies that underlie COVID-19 associated perniois and thrombotic retiform purpura: A case series. *Br. J. Derm.* 2020, 184, 141–150.
 133. Magro, C.M.; Mulvey, J.J.; Laurence, J.; Seshan, S.; Crowson, A.N.; Dannenberg, A.J.; Salvatore, S.; Harp, J.; Nuovo, G.J. Docked severe acute respiratory syndrome coronavirus 2 proteins within the cutaneous and subcutaneous microvasculature and their role in the pathogenesis of severe coronavirus disease 2019. *Hum. Pathol.* 2020, 106, 106–116.
 134. Ko, C.J.; Harigopal, M.; Gehlhausen, J.R.; Bosenberg, M.; McNiff, J.M.; Damsky, W. Discordant anti-SARS-CoV-2 spike protein and RNA staining in cutaneous perniois lesions suggests endothelial deposition of cleaved spike protein. *J. Cutan Pathol* 2021, 48, 47–52.
 135. Bernard, I.; Limonta, D.; Mahal, L.K.; Hobman, T.C. Endothelium Infection and Dysregulation by SARS-CoV-2: Evidence and Caveats in COVID-19. *Viruses* 2021, 13, 29.
 136. Shang, J.; Wan, Y.; Luo, C.; Ye, G.; Geng, Q.; Auerbach, A.; Li, F. Cell entry mechanisms of SARS-CoV-2. *Proc. Natl. Acad. Sci. USA* 2020, 117, 11727–11734.
 137. Benton, D.J.; Wrobel, A.G.; Xu, P.; Roustan, C.; Martin, S.R.; Rosenthal, P.B.; Skehel, J.J.; Gamblin, S.J. Receptor binding and priming of the spike protein of SARS-CoV-2 for membrane fusion. *Nature* 2020, 588, 327–330.
 138. Li, F. Structure, Function, and Evolution of Coronavirus Spike Proteins. *Annu. Rev. Virol.* 2016, 3, 237–261.
 139. Weiss, A.; Jellingsø, M.; Sommer, M.O.A. Spatial and temporal dynamics of SARS-CoV-2 in COVID-19 patients: A systematic review and meta-analysis. *EBioMedicine* 2020, 58, 102916.
 140. Sikora, M.; von Bülow, S.; Blanc, F.E.C.; Gecht, M.; Covino, R.; Hummer, G. Computational epitope map of SARS-CoV-2 spike protein, Supplementary Information, Movie S1. *PLoS Comput. Biol.* 2021, 17, e1008790.

141. Casalino, L.; Gaieb, Z.; Goldsmith, J.A.; Hjorth, C.K.; Dommer, A.C.; Harbison, A.M.; Fogarty, C.A.; Barros, E.P.; Taylor, B.C.; McLellan, J.S.; et al. Beyond Shielding: The Roles of Glycans in the SARS-CoV-2 Spike Protein; supplementary Information. *ACS Cent. Sci.* 2020, 6, 1722–1734.
142. Beniac, D.R.; Andonov, A.; Grudeski, E.; Booth, T.F. Architecture of the SARS coronavirus prefusion spike. *Nat. Struct. Mol. Biol.* 2006, 13, 751–752.
143. Ke, Z.; Oton, J.; Qu, K.; Cortese, M.; Zila, V.; McKeane, L.; Nakane, T.; Zivanov, J.; Neufeldt, C.J.; Cerikan, B.; et al. Structures and distributions of SARS-CoV-2 spike proteins on intact virions. *Nature* 2020, 588, 498–502.
144. Kiss, B.; Kis, Z.; Pályi, B.; Kellermayer, M.S.Z. Topography, Spike Dynamics, and Nanomechanics of Individual Native SARS-CoV-2 Virions. *Nano Lett.* 2021, 21, 2675–2680.
145. Laue, M.; Kauter, A.; Hoffmann, T.; Möller, L.; Michel, J.; Nitsche, A. Morphometry of SARS-CoV and SARS-CoV-2 particles in ultrathin plastic sections of infected Vero cell cultures. *Sci. Rep.* 2021, 11, 3515.
146. Huang, Y.; Yang, C.; Xu, X.-f.; Xu, W.; Liu, S.-w. Structural and functional properties of SARS-CoV-2 spike protein: Potential antiviral drug development for COVID-19. *Acta Pharmacol. Sin.* 2020, 41, 1141–1149.
147. Wrapp, D.; Wang, N.; Corbett, K.S.; Goldsmith, J.A.; Hsieh, C.-L.; Abiona, O.; Graham, B.S.; McLellan, J.S. Cryo-EM structure of the 2019-nCoV spike in the prefusion conformation. *Science* 2020, 367, 1260–1263.
148. Chabert, A.; Hamzeh-Cognasse, H.; Pozzetto, B.; Cognasse, F.; Schattner, M.; Gomez, R.M.; Garraud, O. Human platelets and their capacity of binding viruses: Meaning and challenges? *BMC Immunol.* 2015, 16, 26.
149. Pryzdial, E.L.G.; Lin, B.H.; Sutherland, M.R. Virus–Platelet Associations. In *Platelets in Thrombotic and Non-Thrombotic Disorders: Pathophysiology, Pharmacology and Therapeutics: An Update*; Gresele, P., Kleiman, N.S., Lopez, J.A., Page, C.P., Eds.; Springer International Publishing: New York, NY, USA, 2017; pp. 1085–1102.
150. Stocker, T.J.; Ishikawa-Ankerhold, H.; Massberg, S.; Schulz, C. Small but mighty: Platelets as central effectors of host defense. *Thromb. Haemost.* 2017, 117, 651–661.
151. Hyvärinen, S.; Meri, S.; Jokiranta, T.S. Disturbed sialic acid recognition on endothelial cells and platelets in complement attack causes atypical hemolytic uremic syndrome. *Blood* 2016, 127, 2701–2710.
152. Nissilä, E.; Hakala, P.; Leskinen, K.; Roig, A.; Syed, S.; Van Kessel, K.P.M.; Metso, J.; De Haas, C.J.C.; Saavalainen, P.; Meri, S.; et al. Complement Factor H and Apolipoprotein E Participate in Regulation of Inflammation in THP-1 Macrophages. *Front. Immunol.* 2018, 9, 2701.

153. Soerensen, A.L.; Wandall, H.H.; Patel, S.; Richardson, J.; Italiano, J.; Clausen, H.; Stossel, T.P.; Hartwig, J.H.; Hoffmeister, K.M. Platelets Lacking Sialic Acid Clear Rapidly from the Circulation Due to Ingestion by Asialoglycoprotein Receptor-Expressing Liver Macrophages and Hepatocytes. *Blood* 2006, 108, 1521.
154. Assinger, A. Platelets and Infection—An Emerging Role of Platelets in Viral Infection. *Front. Immunol.* 2014, 5, 649.
155. Kasinrerker, W.; Tokrasinwit, N.; Phunpae, P. CD147 monoclonal antibodies induce homotypic cell aggregation of monocytic cell line U937 via LFA-1/ICAM-1 pathway. *Immunology* 1999, 96, 184–192.
156. Pennings, G.J.; Kritharides, L. CD147 in cardiovascular disease and thrombosis. *Semin. Thromb. Hemost.* 2014, 40, 747–755.
157. Loh, D. The potential of melatonin in the prevention and attenuation of oxidative hemolysis and myocardial injury from cd147 SARS-CoV-2 spike protein receptor binding. *Melatonin Res.* 2020, 3, 380–416.
158. Pushkarsky, T.; Zybarth, G.; Dubrovsky, L.; Yurchenko, V.; Tang, H.; Guo, H.; Toole, B.; Sherry, B.; Bukrinsky, M. CD147 facilitates HIV-1 infection by interacting with virus-associated cyclophilin A. *Proc. Natl. Acad. Sci. USA* 2001, 98, 6360–6365.
159. Rowe, J.A.; Claessens, A.; Corrigan, R.A.; Arman, M. Adhesion of Plasmodium falciparum-infected erythrocytes to human cells: Molecular mechanisms and therapeutic implications. *Expert Rev. Mol. Med.* 2009, 11, e16.
160. Adams, Y.; Kuhnrae, P.; Higgins, M.K.; Ghumra, A.; Rowe, J.A. Rosetting Plasmodium falciparum-infected erythrocytes bind to human brain microvascular endothelial cells in vitro, demonstrating a dual adhesion phenotype mediated by distinct P. falciparum erythrocyte membrane protein 1 domains. *Infect. Immun.* 2014, 82, 949–959.
161. Arman, M.; Rowe, J.A. Experimental conditions affect the outcome of Plasmodium falciparum platelet-mediated clumping assays. *Malar. J.* 2008, 7, 243.
162. Deroost, K.; Pham, T.T.; Opdenakker, G.; Van den Steen, P.E. The immunological balance between host and parasite in malaria. *FEMS Microbiol. Rev.* 2016, 40, 208–257.
163. Choi, Y.K.; Cao, Y.; Frank, M.; Woo, H.; Park, S.-J.; Yeom, M.S.; Croll, T.I.; Seok, C.; Im, W. Structure, Dynamics, Receptor Binding, and Antibody Binding of the Fully Glycosylated Full-Length SARS-CoV-2 Spike Protein in a Viral Membrane. *J. Chem. Theory Comput.* 2021, 17, 2479–2487.
164. Lardone, R.D.; Garay, Y.C.; Parodi, P.; de la Fuente, S.; Angeloni, G.; Bravo, E.O.; Schmider, A.K.; Irazoqui, F.J. How glycobiology can help us treat and beat the COVID-19 pandemic. *J. Biol. Chem.* 2021, 296, 100375.

165. Bharara, R.; Singh, S.; Pattnaik, P.; Chitnis, C.E.; Sharma, A. Structural analogs of sialic acid interfere with the binding of erythrocyte binding antigen-175 to glycophorin A, an interaction crucial for erythrocyte invasion by *Plasmodium falciparum*. *Mol. Biochem. Parasitol.* 2004, 138, 123–129.
166. Jaskiewicz, E.; Jodłowska, M.; Kaczmarek, R.; Zerka, A. Erythrocyte glycophorins as receptors for *Plasmodium* merozoites. *Parasites Vectors* 2019, 12, 317.
167. Halbhuber, K.J.; Gliesing, M.; Stibenz, D.; Makovitzky, J. Topo-optical investigations of the human erythrocyte glycocalyx-age related changes. *Histochemistry* 1984, 81, 187–193.
168. van Oss, C.J.; Absolom, D.R. Zeta potentials, van der Waals forces and hemagglutination. *Vox Sang.* 1983, 44, 183–190.
169. Pretini, V.; Koenen, M.H.; Kaestner, L.; Fens, M.H.A.M.; Schiffelers, R.M.; Bartels, M.; Van Wijk, R. Red Blood Cells: Chasing Interactions. *Front. Physiol.* 2019, 10.
170. Fernandes, H.P.; Cesar, C.L.; Barjas-Castro Mde, L. Electrical properties of the red blood cell membrane and immunohematological investigation. *Rev. Bras. Hematol Hemoter* 2011, 33, 297–301.

Retrieved from <https://encyclopedia.pub/entry/history/show/50758>